A GLR algorithm to detect and exclude up to two simultaneous range failures in a GPS/Galileo/IRS case

Audrey Giremus, Anne-Christine Escher

▶ **To cite this version:**

Audrey Giremus, Anne-Christine Escher. A GLR algorithm to detect and exclude up to two simultaneous range failures in a GPS/Galileo/IRS case. ION GNSS 2007, 20th International Technical Meeting of the Satellite Division of The Institute of Navigation, Sep 2007, Fort Worth, United States. pp 2911-2923. hal-01022192

HAL Id: hal-01022192

https://enac.hal.science/hal-01022192v1

Submitted on 31 Oct 2014

HAL is a multi-disciplinary open access archive for the deposit and dissemination of scientific research documents, whether they are published or not. The documents may come from teaching and research institutions in France or abroad, or from public or private research centers.

L'archive ouverte pluridisciplinaire **HAL**, est destinée au dépôt et à la diffusion de documents scientifiques de niveau recherche, publiés ou non, émanant des établissements d'enseignement et de recherche français ou étrangers, des laboratoires publics ou privés.

A GLR Algorithm to Detect and Exclude up to Two Simultaneous Range Failures in a GPS/Galileo/IRS Case

Audrey Giremus, *Université de bordeaux, France*
Anne-Christine Escher, *Ecole Nationale de l'Aviation Civile, France*

BIOGRAPHY

Audrey Giremus received the engineer degree and the Ph.D. degree in signal processing from SUPAERO (ENSAE) in Toulouse, France. She is currently an associate professor at the University of Bordeaux. Her research interests include statistical signal processing and optimal filtering techniques applied to navigation and localization.

Anne-Christine ESCHER graduated as an electronics engineer in 1999 from the ENAC in Toulouse, France. Since 2002, she has been working as an associated researcher in the signal processing lab of the ENAC. She received her Ph.D. in 2003.

ABSTRACT

The advent of new satellite signals with Galileo L1/E5 and modernized GPS L5 is expected to significantly improve navigation performance both in terms of accuracy and integrity monitoring. On the one hand, dual frequency measurements will allow to remove most of the ionospheric error degrading the pseudoranges. On the other hand, the opportunity of using two constellations of satellites for positioning will significantly improve the fault detection and exclusion (FDE) function availability by increasing the redundancy among the measurement sources. This enhancement comes at the expense an increased computational complexity when applying the exisiting integrity monitoring schemes. This paper focuses on Aircraft-based Autonomous Integrity Monitoring (AAIM) techniques where the GPS and Galileo are integrated with an Inertial Reference System (IRS). In this framework, we present an alternative approach for fault detection and exclusion based on the Generalized Likelihood Ratio algorithm which is well-known in the Control community. A few adaptations to the classical formulation are proposed to make the algorithm compliant with civil aviation requirements.

INTRODUCTION

While only GPS L1 signals are available, GPS/IRS hybridization is a good candidate to fulfill stringent civil aviation requirements. When the integrity of GPS measurements is ensured, they can be used to compensate for slow IRS drifts thereby yielding a tighter position solution. This can be performed in a tightly coupled manner by means of a Kalman filter. In return, calibrated IRS may ensure coasting while maintaining short-term accuracy. Aircraft-based Autonomous Integrity Monitoring (AAIM) approaches have been proposed to detect errors at the level of the hybridization filter. They have been shown to improve availability with respect to RAIM by taking advantage of the synergy between GPS and IRS measurements to detect slowly growing disturbances.

The advent of Galileo offers new opportunities: it is expected that in 2016, the GPS and Galileo satellite constellations broadcasting both L1/L5 and L1/E5b signals, respectively, will be operational. In this context, the relevance of GNSS/IRS hybridization AAIM algorithms can be questioned as the GPS/Galileo combination is expected to enhance the ability of radio-navigation receivers to detect and exclude faulty satellites by increasing redundancy among measurement sources. Besides, dual-frequency measurements will allow correcting for the ionospheric delays that degrade the GPS or Galileo pseudorange measurements. Hence, once the main part of the measurement noise is removed, the GNSS estimates of the aircraft dynamics are expected to be far more accurate, enhancing the feasibility of stringent operations like APV-I with RAIM. On the other side, the GNSS/IRS hybridization AAIM algorithms will become more complex and more costly in terms of computational and material resources, to cope with the dual GPS/Galileo constellation. However, hybridization with IRS is still of

interest for safety critical operations APV-I and APV-II as IRS aiding may improve robustness against interferences which are among the most penalizing sources of errors. Besides, GNSS/IRS could remain as an alternative to satellite navigation when it encounters some degraded scenarios (loss of one frequency for instance). It is consequently worth studying the impact of a dual constellation on hybridization algorithms.

In GPS/IRS-based AAIM algorithms, the fault detection and exclusion (FDE) functions are classically performed by means of a bank of Kalman filters, each one taking into account a subset of satellites. All but one sub-filter use at least a faulty measurement, which makes anomaly identification possible. In this context, the potential improvement of performance due to the combination of GPS and Galileo constellations should be carefully balanced with the increased complexity of the hybridization algorithms. Moreover, the effects of multiple range failures degrading simultaneous measurements may be considered to be significant for the above mentioned critical operations as they require tight alert limits. A straightforward solution consists in adding a layer of sub-filters, possibly leading to unrealistic architectures. For this reason, it is worth studying alternative algorithms which would be less consuming in terms of computational resources such as the Generalized Likelihood Ratio (GLR), which is widely applied to perform fault diagnosis among the signal processing community.

The GLR has been developed as an extension of the Kalman filter to detect abrupt changes affecting dynamic systems. The monitoring is performed at the level of the Kalman innovations. The GLR takes advantage of the fact that the impact of a measurement error on the Kalman filter innovations can be expressed analytically. Thus, it suffices to maintain only the main Kalman filter while computing in parallel the signatures of the potential failures on the state estimates and the measurement predictions. It should be noted that the GLR not only detects failures but also estimates their magnitude and their time of occurrence. The risk that an anomaly may contaminate slowly the Kalman filter outputs without being spotted is consequently reduced. This paper investigates applying the GLR in a civil aviation context. Some modifications to the basic formulation are proposed including an extension to cover the case of slowly growing errors as well as the derivation of protection level formula.

The paper is organized in 4 parts. The first section is dedicated to AAIM techniques. It presents the principles of GNSS/IRS hybridization, and gives a hint on the concepts underlying integrity monitoring techniques. Existing FDE approaches are thus introduced in a few words. The 2nd section describes the GLR and discusses its properties. Then, some modifications to the standard implementation are proposed in the 3rd section to obtain a civil aviation compliant algorithm. Finally, a performance analysis is conducted by means of extensive simulations. The performance in terms of integrity monitoring and availability is assessed and compared to those of a weighted-LSR RAIM and to the Multiple Solution Separation (MSS) algorithm proposed by Brenner [1]-[2]. Several configurations have been studied, including mono-frequency or dual frequency measurements, and mono-constellation or combined constellation.

AAIM APPROACHES

The performance of standalone GPS in terms of accuracy and more particularly in terms of integrity monitoring, availability and continuity do not suit ICAO recommendations to be certified as a primary means of navigation. Onboard commercial aircrafts, the GPS is thus used in combination with other sensors such as classically IRS or radio-altimeters. The use of IRS is motivated by their synergy with GPS. Despite a very good short-term accuracy, they suffer from long-term estimation error drifts. On the contrary, the GPS error is bounded over time and only depends on the receiver environment and relative geometry with respect to the satellites. The price to pay is a sensitivity to external perturbations such as multipath effects and interferences. Various coupling architectures have been considered but we focus herein on a tight hybridization.

Tight coupling consists in taking advantage of GPS measurements to compensate for IRS drifts and calibrate IRS sensors. In return, the calibrated IRS provides accurate motion estimates during GPS outages. The main interest of this architecture is that slowly varying IRS estimation errors and sensor biases are estimated rather than directly the motion parameters such as the velocity or the position. The robustness towards abrupt changes of dynamics of the aircraft is thereby increased. A Kalman filter is usually implemented to solve the estimation problem.

GPS/IRS hybridization model

When a tight GPS/IRS coupling is applied, the state vector is composed of the INS estimation errors and the various sensor biases, both those affecting INS and GPS measurements. This state vector, at time t, is denoted hereafter x_t and is defined as

$$x_t = \left[\delta p_t, \delta v_t, \rho_t, b_t^a, b_t^g, b_t, \dot{b}_t\right],$$

where:

- δp_t and δv_t are the IRS positioning and earth relative velocity errors, respectively. The frame of coordinates in which they are expressed depends on the application and thus is voluntarily left unspecified herein. Usually, the navigation frame whose axes

point toward the local vertical, North and East is used by sake of convenience.

- ρ_t is the INS attitude estimation error vector, where the aircraft attitude is classically defined by 3 so-called Euler angles (roll, pitch, yaw).
- b_t^a and b_t^g represent the accelerometer and gyrometer biases, respectively.
- b_t and $\dot{b}_t$ are the GPS receiver clock bias and drift

Many inertial error models are available in the literature depending on the chosen frame of reference and the considered sensor error models. They are all obtained by linearizing the IRS equations, which relate the inertial sensor measurements to the true motion parameters, around the IRS estimates. The GPS/IRS state equations have therefore the proper linear form for a Kalman filtering:

$$x_{t+1} = F_t x_t + v_t,$$

where v_t is a white Gaussian noise whose covariance matrix Q_t depends on the class of the IRS sensors and on the GPS receiver clock model. Detailed expressions for the state matrices F_t and Q_t can be found in many textbooks, including for instance [9].

The measurement equation non linearly relates the GPS measurements to the error states as follows:

$$z_t = h_t(x_t) + w_t,$$

with w_t a white Gaussian noise whose covariance matrix R_t depends on the GPS measurement error budget. The GPS measurements are the code pseudo-ranges. Geometrically, they represent the distance between the observed satellite and the receiver, corrupted by the receiver clock bias. The i[th] component of the measurement vector z_t consequently satisfies:

$$z_t(i) = \left\| p_t - p_t^i \right\| + b_t + w_t$$
$$z_t(i) = \left\| \delta p_t + \left(p_t^{ins} - p_t^i \right) \right\| + b_t + w_t$$

where p_t^i, p_t and p_t^{ins} denote the i[th] satellite position, the actual mobile position and its IRS estimate respectively, all resolved in the same frame of coordinates.

This equation is non linear, hence must be linearized to allow for a Kalman solution to the navigation problem. Usually, it is replaced by the following 1[st] order Taylor expansion at each recursion of the Kalman filter:

$$y_t = z_t - h_t(\hat{x}_{t|t-1}) + H_t \hat{x}_{t|t-1} + w_t = H_t x_t + w_t,$$

with $\hat{x}_{t|t-1}$ the latest estimate of the state vector and H_t the matrix of the partial derivates of h_t with respect to the state parameters.

The state space model associated to the hybrid GPS/IRS navigation system consequently takes the form:

$$\begin{aligned} x_{t+1} &= F_t x_t + v_t \\ y_t &= H_t x_t + w_t. \end{aligned} \qquad (1)$$

It should be noted that this model also holds for GPS/Galileo/IRS hybridization, except that the measurement vector is augmented with Galileo pseudo-ranges and the subsequent components of the matrix R_t depend on the Galileo error budget. In this study it is assumed that the GGTO has been broadcasted in the Galileo message. Before presenting the Kalman solution to the estimation problem defined by (1), let us focus on the necessary adjustments when using dual-frequency or mono-frequency measurements. As recommended in the appendix R to DO229D [3], GNSS measurement errors have been modeled as time-correlated processes that can mislead the FDE algorithm and result in false detections. The solution consists then in augmenting the state vector to estimate these correlated errors jointly with the navigation parameters and sensor biases. When only mono-frequency measurements are available, the ionospheric error that is predominant is modeled as a 2[nd] order Markov process [4]. As for the dual-frequency measurements, they allow to remove the ionospheric delay. In this case the remainder of the measurement error can be merely represented by a 1[rst] order Markov process and the variance of the measurement noise is decreased accordingly in the matrix R_t.

In this framework, the Kalman filter recursively computes the best state vector estimate at time t, denoted $\hat{x}_{t|t}$, in the sense that it minimizes the mean square estimation error. Let us recall the Kalman equations to introduce the notations used throughout this paper:

$$\hat{x}_{t+1|t} = F_t \hat{x}_{t|t}$$
$$P_{t+1|t} = F_t P_t F_t^T + Q_t$$
$$\varepsilon_{t+1} = y_{t+1} - H_{t+1} \hat{x}_{t+1|t}$$
$$K_{t+1} = P_{t+1|t} H_{t+1}^T (H_{t+1} P_{t+1|t} H_{t+1}^T + R_{t+1})^{-1}$$
$$\hat{x}_{t+1|t+1} = \hat{x}_{t+1|t} + K_{t+1} \varepsilon_{t+1}$$
$$P_{t+1} = (I - H_{t+1} K_{t+1}) P_{t+1|t}$$

In these equations, ε_{t+1} is called the Kalman innovation and is expressed as the difference between the actual measurement vector and the predicted one. According to the Kalman filter properties, the sequence of innovations

is a white Gaussian noise. We hereafter denote its covariance matrix S_{t+1}:

$$S_{t+1} = E(\varepsilon_{t+1}\varepsilon_{t+1}^T) = H_{t+1}P_{t+1|t}H_{t+1}^T + R_{t+1}.$$

Fault detection and exclusion objectives and techniques

The Kalman filter yields a good solution to the estimation problem provided the state space model properly describes the system behavior. In particular, unexpected errors degrading the measurements will gradually drag off the estimates.

Usually, algorithms are calibrated to protect the user against a major satellite failure. It is defined as a ranging error exceeding 30m whose probability is $10^{-4}/fh$ and which is assumed to affect only one of the visible GPS satellite at a time. In fact, on-board integrity algorithms are able to protect the user against any single failure that would have a probability lower than $10^{-4}/fh$ but larger than the required integrity risk. The occurrence of simultaneous major failures is very low, and despite the occurrence of any type of ranging failures lower than 30m is not standardized, the single failure assumption was sufficient for the current targeted phases of flight, up to NPA, as their alert limit is large enough (larger than 556.5m) [10]. This major failure results in non centered measurement errors, typically modeled as a bias or a ramp. Assuming such a measurement failure occurs at time k, the state space model (1) becomes:

$$\begin{aligned} x_{t+1} &= F_t x_t + v_t \\ y_t &= H_t x_t + w_t + \nu\Gamma(t-k), \end{aligned} \qquad (2)$$

where the function $\Gamma(t-k)$ depends on the type of error as specified in Table 1 and ν is the vector of the error magnitudes, which is multi-dimensional to cover the case of multiple simultaneous failures.

Step error	$\Gamma(t-k) = \begin{cases} 1 \text{ if } t \geq k, \\ 0 \text{ otherwise.} \end{cases}$
Ramp error	$\Gamma(t-k) = \begin{cases} t-k \text{ if } t \geq k, \\ 0 \text{ otherwise.} \end{cases}$

Table 1: failure specifications.

From now on, the outputs of the Kalman filter assuming a measurement failure at time k will be denoted $\hat{x}_{t|t}[k]$, $\varepsilon_t[k]$ and $\hat{x}_{t+1|t}[k]$, respectively.

Integrity monitoring techniques aim at detecting the presence of faulty measurements and excluding them (FDE function) to ensure the continuity of the navigation service in accordance with ICAO false alarm, missed alert and failed exclusion requirements. For that purpose, the navigation algorithms are extended to include statistical tests yielding for instance the well-known AIME [5] and the MSS approaches in the context of GPS/IRS coupling. The AIME monitors the whiteness of the Kalman innovations to detect potential failures whereas the second one proceeds by comparing the full-measurement solution to solutions based on subsets of the collected measurements. Whatever the algorithm, the exclusion step requires a comparison of the current solution with a fault-free solution. For that purpose, assuming a single faulty measurement at a time, a bank of parallel Kalman sub-filters using all but one of the available measurements must be maintained jointly with the main Kalman filter. In this way, one of the sub-filters is sure to exclude the faulty measurement and thus compute the fault-free solution. If the scenario of two simultaneous failures becomes likely, an additional layer of sub-filters excluding 2 of the collected measurements is required to perform FDE. Integrity is thus ensured at the price of a sometimes prohibitive computational cost, in particular when the number of satellite measurements is high. The advent of modernized GPS and Galileo has consequently motivated the development of less resource-consuming FDE algorithms.

This paper studies the applicability of the Generalized Likelihood Ratio (GLR) to civil aviation navigation. First, only the case of abrupt step failures is investigated. Then, extensions to the GLR are discussed to meet civil aviation constraints.

THE GENERALIZED LIKELIHOOD RATIO TECHNIQUE

The GLR has long been applied in the field of Automatic and Control to detect possible component failures in a system. First introduced by Willsky [6], this algorithm has become increasingly popular for being readily applicable to any dynamical system provided its state is estimated by Kalman filtering. The detection of abrupt changes affecting the components of the state vector, or equivalently the components of the observation vector, is performed by sequentially applying a likelihood ratio (LR) hypothesis testing.

The GLR is an appealing alternative to existing FDE algorithms for naturally coping with multiple simultaneous failures, but also for being robust to disturbances of small magnitude. Indeed, the GLR algorithm not only explores any possible change direction but also any possible change time up to the current time. In this way, the detection of small systematic measurement errors that would slowly contaminate the Kalman estimates is made possible. Furthermore, the key idea of the GLR is to make explicit the impact of a state or measurement mean jump on the Kalman filter estimates. In this way, computational power can be saved since there is no need to run as many Kalman filters as

possible jump hypotheses: it suffices to compute the signature of the failures on the filter outputs. The main flaw of this approach is that no fault-free solution is maintained. Therefore, whenever an anomaly is detected, a compensation step is necessary to remove the induced errors on the Kalman filter estimates. In this part, we briefly recall the principles of the GLR algorithm when applied to the model defined by (2) with the step error.

At time t, the issue at hand is to decide between the following competing hypotheses:

- H_0 : no measurement failure has occurred,
- $H_1(k,\nu)$: a mean jump of amplitude ν has occurred at time $k \le t$.

To begin with, we assume the jump vector ν is known. In this context, likelihood ratios (LR) have been proved to be the most efficient statistic tests according to the Neyman-Pearson lemma as stated by theorem 3.1. in [7]. They proceed by comparing the following test statistic to a threshold to make the proper decision:

$$l_t(k,\nu) = \frac{p(y_{1:t}|H_1(k,\nu))}{p(y_{1:t}|H_0)}.$$

This LR can be expressed as a function of the Kalman filter innovations only, as follows:

$$l_t(k,\nu) = \frac{\prod_{l=k}^{t} p(\varepsilon_l|H_1(k,\nu))}{\prod_{l=k}^{t} p(\varepsilon_l|H_0)} = \frac{\prod_{l=k}^{t} p(\varepsilon_l[k])}{\prod_{l=k}^{t} p(\varepsilon_l)}. \quad (3)$$

For being easier to handle, the log likelihood ratio $L_t(k,\nu) = 2\log l_t(k,\nu)$ is usually used instead, where the factor 2 is introduced for notational convenience. If $L_t(k,\nu) \ge h$, h standing for the test threshold, then the hypothesis $H_1(k,\nu)$ is validated. Guidelines on the choice of h are provided below.

This decision rule cannot be applied straightforwardly since both the change time k and the mean jump vector ν are unknown. Assuming the vector ν is available, the best change time can be chosen as the one yielding the highest value of the log likelihood ratio. As for the dependence of the decision variable on the jump vector, the GLR overcomes this difficulty by replacing ν by its maximum likelihood estimate. Indeed, The algorithm relies on the observation that the Kalman filter innovations under hypothesis $H_1(k,\nu)$ linearly depend on the mean jump vector ν. Thus, they can be expressed as follows:

$$\varepsilon_l[k] = \varphi_l^T[k]\nu + \varepsilon_l \text{ , for } k \le l \le t \text{ , } (4)$$

where $\varphi_l^T[k]$ is the regression matrix or the failure signature matrix for the innovations, which can be computed recursively as:

$$\varphi_{l+1}^T[k] = I - H_{l+1}F_l\mu_l[k],$$

where $\mu_l[k]$ is the failure signature for the Kalman state estimates satisfying:

$$\mu_l[k] = F_{l-1}\mu_{l-1}[k] + K_l\varphi_l^T[k].$$

It follows that the Kalman filter innovations can be considered as observations of the unknown jump vector ν, corrupted by the white noise process ε_l. Thus, a weighted least-square (WLS) estimate of this vector can be obtained as

$$\hat{\nu}[k] = R_t[k]^{-1} f_t[k],$$

with:

- $R_t[k] = \sum_{l=k}^{t} \varphi_l[k] S_l^{-1} \varphi_l^T[k]$,
- $f_t[k] = \sum_{l=k}^{t} \varphi_l[k] S_l^{-1} \varepsilon_l[k]$.

Using this expression in (3) and (4) then yields the following simple expression for the test statistic:

$$L_t(k,\hat{\nu}[k]) = f_t^T[k] R_t[k]^{-1} f_t[k].$$

The decision rule stated above can finally be applied.

To sump up, the whole GLR algorithm proceeds as follows at time t:

1) For each change time candidate k, computation of the corresponding WLS estimate of the measurement mean jump vector $\hat{\nu}[k]$.
2) Use of this value to obtain an approximate log-LR test statistic $L_t(k,\hat{\nu}[k])$.
3) The best candidate change time is selected as:
$$\hat{k} = \arg\max_k L_t(k,\hat{\nu}[k]).$$
4) The corresponding statistic $L_t(\hat{k},\hat{\nu}[\hat{k}])$ is used to make the decision. With no loss of generality, we use $s_t = \sqrt{L_t(\hat{k},\hat{\nu}[\hat{k}])}$ as test variable in this paper for convenience. This formulation is indeed equivalent and makes the derivation of protection levels easier as shown in the last section.
5) Finally, once detected a system anomaly, the GLR takes advantage of the regression matrices to compensate for the errors introduced on the Kalman outputs. The reader can refer to [Willsky] for further details.

Before discussing the possibilities to use such an algorithm in a civil aviation context, let us make a few comments on the implementation. Firstly, it should be noticed that the search for the best occurrence time is usually limited to a sliding window of size L to prevent the computational cost to increase with time. L is chosen to make the balance between the computational complexity and the detection performance. Secondly, the inversion of the matrix $R_t[k]$ can be avoided provided a weighted recursive least square (RLS) scheme is applied to estimate $\hat{\nu}[k]$. Thus, by comparison with existing integrity monitoring techniques, the GLR requires L parallel RLS filters instead of a bank of Kalman filters, hence is less costly.

Finally, the test threshold h can be adjusted to ensure a given false alarm rate. It suffices to notice that under the null hypothesis, the square of the test variable s_t is χ^2-distributed with as many degrees of freedom as components of the jump vector ν. The convenient threshold can consequently be found in standard statistical tables.

ADAPTATION TO CIVIL AVIATION CONSTRAINTS

Even if the GLR is widely acknowledged as a powerful surveying algorithm, it cannot be applied in its current form to monitor an aircraft navigation service integrity. In this section, we propose a few adaptations to the GLR formulation so that the algorithm becomes compliant with the civil aviation requirements. In particular, the following issues are addressed:

- the algorithm should be able to deal with ramp errors as well as with step errors.
- The error sources should be identified and excluded so that navigation goes on safely with the set of error-free measurements.
- The performance of the integrity monitoring scheme should be assessed by means of protection level computations, for instance.

Our contribution is therefore threefold. Firstly, we propose to use fixed direction test variables to jointly detect a failure and identify its direction. Secondly, we extend the standard GLR formulation to handle ramp errors. Finally, protection levels formula are derived that can take into account slowly growing estimation errors due to undetected measurement biases.

Error identification using fixed direction test variables

Integrity monitoring algorithms aim not only at detecting measurement failures but also at identifying and excluding the faulty measurements to ensure the continuity of the navigation service.

A solution to identify the faulty components of the measurement vector consists in using fixed direction test variables for which the failure is enforced to lie in a given direction, as already proposed in [8]. Under this constraint, the scope of the possible measurement failures is limited to mean jumps that can be factored as:

$$\nu = T\nu_T ,$$

where T is a matrix which projects the errors on a given set of measurements and ν_T is the vector of the mean jump amplitudes along the failure directions.

Assuming one failure at a time, projection vectors of the form:

$$T_i = [0,\cdots,1,\cdots 0]^T \text{ for } i = 1,\cdots,n_y ,$$

are considered, where n_y is the dimension of the measurement vector. They are null vectors except for the ith component which is equal to 1. In this case, the GLR only searches for mean jump vectors that can be written:

$$\nu = T_i\nu_i ,$$

with ν_i a scalar corresponding to the failure magnitude.

Then, the GLR setting remains the same except that in addition to testing all possible change times, the algorithm searches also the most likely failure directions. For that purpose, the algorithm computes an estimate of the mean jump amplitude $\hat{\nu}^i[k]$ and thereby a test statistic for each time of failure occurrence and direction candidate couple (k,i). It is expressed as:

$$l_t^{\,i}(k,\hat{\nu}^i[k]) = f_t^i[k]^T R_t^i[k]^{-1} f_t^i[k] \quad (5)$$

with

$$R_t^i[k] = \sum_{l=k}^{t} T_i^T \varphi_l[k] S_l^{-1} \varphi_l^T[k] T_i ,$$

$$f_t^i[k] = \sum_{l=k}^{t} T_i^T \varphi_l[k] S_l^{-1} \varepsilon_l[k] .$$

A double maximization gives the best couple:

$$(\hat{k},\hat{\imath}) = \arg\max_{(k,i)} l_t^{\,i}(k,\hat{\nu}^i[k]) .$$

The associated test variable $s_t = \sqrt{l_t^{\,\hat{\imath}}(\hat{k},\hat{\nu}^{\hat{\imath}}[\hat{k}])}$ is then compared to the test threshold to validate the failure hypothesis. In this way, the detection and identification processes are carried out at the same time. If the test flags an anomaly then navigation goes on with all but the ith satellite measurement.

This structured testing can be readily extended to handle multiple failures. In the case of two simultaneous range failures, mean jump vectors of the form:

$$\nu = T_{ij}\nu_{ij} ,$$

are considered, where T_{ij} is a null matrix of dimension $n_y \times 2$ whose elements $T_{ij}(i,1)$ and $T_{ij}(j,2)$ are equal to 1, and ν_{ij} is a vector of size 2.

It should be noticed that this approach does not increase too much the computational complexity since the regression matrices $\varphi_l[k]$ can be computed independently of the considered failure directions. Besides, the GLR parallel RLS filters estimate a scalar or a vector of size 2 instead of the whole mean jump vector ν.

Detection/Exclusion of ramp failures

Little changes are required so that the GLR algorithm can cope with ramp errors. Because of the model linearity with respect to both the state vector and the vector ν, we can postulate that the Kalman filter outputs assuming a ramp error beginning at time k on the ith measurement still take the form:

$$\varepsilon_t^i[k] = \varphi_t^T[k]T_i\nu_i + \varepsilon_t,$$
$$\hat{x}_{t|t}^i[k] = \mu_t[k]T_i\nu_i + \hat{x}_{t|t},$$

except that ν now denotes the slope of the ramp failure. However, the regression matrix formula should be modified to take into account the error linear growth. They become:

$$\varphi_t^T[k] = (t-k)I - H_tF_{t-1}\mu_{t-1}[k]$$
$$\mu_t[k] = F_{t-1}\mu_{t-1}[k] + K_t\varphi_t^T[k].$$

The GLR formulation can thus be adapted so that either step or ramp failures can be detected. However, the integrity monitoring algorithm should apply without prior assumption on the type of failure. A simple rule can be used to make the GLR decision flexible. We propose to modify the GLR so that the regression matrices for both ramp and step errors are computed in parallel as well as the resulting log-likelihood ratios. The algorithm then selects the most likely failure type jointly with the time of occurrence and the anomaly direction as the ones yielding the highest value of the test statistics. The remainder of the algorithm remains is unchanged.

Protection levels

Once FD is processed, one must ensure of the algorithm performance with regards to the ICAO integrity requirement. FD performance is usually assessed by means of protection levels that are compared to the required alert limits. They are upper bounds on the positioning error, either in the horizontal plane or along the vertical axis, that cannot be exceeded without a failure being detected by the navigation system with the probability $1 - P_{MD}$, where P_{MD} is the missed detection rate.

Thus, protection levels represent the impact in the position domain of the minimum detectable bias. Knowing that the position error jointly depends on the measurement uncertainty and the satellite constellation geometry that varies through time and location, protection levels are usually expressed as:

$$xPL = xSLOPE_{\max} \times s_{bias}, \quad (6)$$

where

- x stands for V or H for the vertical axis or the horizontal plane, respectively,
- s_{bias} is the projection in the test variable space of the minimum detectable bias in accordance with P_{MD},
- and $xSLOPE_{\max}$ is a factor depending on the satellite constellation geometry.

In this section, we propose protection level formula to measure the integrity monitoring performance of the GLR-based FDE algorithm. Previous material on the subject can be found in [8]. The main contribution of this paper consists in taking into account the GLR detection delay in the protection level computation. Indeed, with the varying satellite geometry, undetected past failures may impact the position estimates more strongly than current failures. This is the reason why the GLR searches for any failure time in a sliding window and why delayed impact of range biases should be considered in the protection level formula. Hereafter, the assumption of a single failure at a time is made and the structured test variable formulation of the GLR is considered.

Assuming all measurements are noise-free and a bias ν appears at time k on the ith measurement, the induced positioning error at time $t \geq k$ is linearly related to ν according to the formula:

$$dx_t^i[k] = x_t - \hat{x}_{t|t}^i[k] = \mu_t[k]T_i\nu_i.$$

By processing separately the horizontal and vertical components of the position, we obtain:

$$dR_t^i[k] = \left\|\mu_t^H[k]T_i\right\|\nu_i \quad \text{for the horizontal error (7)}$$

$$dh_t^i[k] = \left\|\mu_t^V[k]T_i\right\|\nu_i \quad \text{for the vertical error (8)}$$

where $\mu_t^V[k]$ and $\mu_t^H[k]$ are the sub-matrices of $\mu_t[k]$ associated respectively to the vertical and to the horizontal position elements.

Besides, the impact of the measurement bias on the test variable is also linear. Indeed under the noise free assumption, the innovation in the presence of the mean jump becomes:

$$\varepsilon_l^i[k] = \varphi_l^T[k] T_i \nu_i, \forall l \geq k .$$

By using this expression in (5), it follows that the resulting deviation of the test variable is:

$$ds_t^i[k] = \nu \sqrt{T_i^T \left(\sum_{l=k}^{t} \varphi_l[k] S_l^{-1} \varphi_l^T[k] \right) T_i} \quad (9)$$

By combining equation (9) with equation (7) or (8) to remove the bias term, a linear relationship between the positioning error and the induced test variable deviation can be established. Thus,

$$dR_t^i[k] = HSLOPE[k,i] \times ds_t^i[k]$$
$$dh_t^i[k] = VSLOPE[k,i] \times ds_t^i[k] \quad \text{, with}$$

$$xSLOPE[k,i] = \frac{\left\| \mu_t^x[k] T_i \right\|}{\sqrt{T_i^T \left(\sum_{l=k}^{t} \varphi_l[k] S_l^{-1} \varphi_l^T[k] \right) T_i}}$$

On the basis of this result, conservatives values of the protection level can be computed by replacing $HSLOPE_{\max}$ and $VSLOPE_{\max}$ in (6) by:

$$HSLOPE_{\max} = \max_{\substack{t-L \leq k \leq t \\ i}} \left(HSLOPE[k,i] \right),$$

$$VSLOPE_{\max} = \max_{\substack{t-L \leq k \leq t \\ i}} \left(VSLOPE[k,i] \right).$$

In this expression, we recall that L is the size of the analyzing window.

It should be noted that this derivation differs from [8] since the $xSLOPE$ values jointly depend on the failure direction and the time of occurrence. The computations of the $xSLOPE_{\max}$ factors consequently involve a double maximization over k and i. As for s_{bias}, it is computed classically to ensure a given missed detection probability. When a failure has occurred, the square of the test variable s_t satisfies a non-centered χ^2-distribution. The value of the corresponding non-centrality parameter λ can be adjusted so that the hypothesis test meets the required missed detection probability. Then, s_{bias} is obtained as:

$$s_{bias} = \sqrt{\lambda} .$$

By applying (6), small values of the protection levels are obtained so that they can be exceeded due to noise only. Proper $xPLs$ should therefore take into account the rare normal performance case. They can be computed as:

$$HPL = \max\left(HPL_0, HSLOPE_{\max} s_{bias} \right),$$
$$VPL = \max\left(VPL_0, VSLOPE_{\max} s_{bias} \right),$$

with $xPL_0 = 5.33 \times \sigma_x$, σ_x being the standard deviation of the positioning error estimate either along the vertical axis or in the horizontal plane

SIMULATION RESULTS

In order to assess the performance of the GLR as an integrity monitoring algorithm, we have conducted several simulations corresponding to different GPS-Galileo constellation settings:

- GPS L1 or L1/L5,
- Galileo L1/E5,
- GPS+Galileo L1/E5-L5.

The scope of this paper is limited to AAIM (Aircraft Autonomous Integrity Monitoring) approaches so that the satellite system is coupled with an IRS in the considered simulation scenarios. A tight integration has been applied for making the most of GPS/IRS synergy. The obtained results are compared with those achieved by classical FDE algorithms such as:

- the Multiple Solution Separation (MSS) [1],
- the weighted Least-Square Residual RAIM. In this case, the FDE is performed previous to the GPS/Galileo-IRS hybridization filter which takes as inputs only the GPS/Galileo measurements that have been monitored fault-free.

The AIME has not been tested due to the lack of details on its exact implementation in the literature.

The performance of the different approaches has been studied in terms of availability and detection/exclusion capability by computing protection levels, mean detection/exclusion delays and mean error sizes at detection/exclusion.

It should be noticed that when coupling GPS or Galileo with IRS, the FDE level of performance does not depend only on the location of the GNSS receiver on earth. For this reason, we cannot provide availability results on a world-wide grid map. We propose instead to consider a typical flight trajectory and compute pointwise protection levels.

Simulation setting

The simulations have been carried out with Matlab. The considered trajectory is a Toulouse/Paris flight path of duration 6000s which has been simulated from recorded attitude and position data. A GNSS software computes the GPS and/or Galileo pseudo-ranges all along this trajectory. The GPS and Galileo simulated constellations are represented on Fig.1. This software can provide mono-frequency as well as dual-frequency measurements. According to appendix R to DO229D, all the noise sources have been generated as correlated processes as explained previously.

As for the IRS measurements, the gyrometer and accelerometer errors have been modeled as random walks and biases. The following sensor specifications have been considered:

- Gyrometer random walk standard deviation: $1°/h$.
- Accelerometer random walk standard deviation: $25\ \mu g$.

The vertical drift of the IRS is slowed down thanks to a baro-altimeter aiding. The implemented baro-inertial architecture is a third order loop and we have assumed a 200 ft standard deviation for the barometric error.

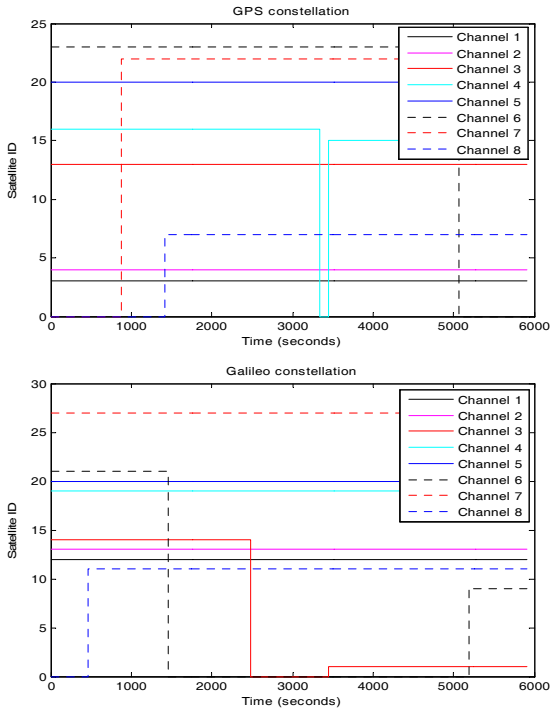

Fig 1 : simulated GPS and Galileo constellations.

Performance requirements

In this study, the performance analysis of the integrity monitoring algorithms is conducted only for the most stringent phases of flight, i.e. APVI and APV II. Thus, the value of the false detection/exclusion rates required to compute the FDE function decision thresholds as well as the value of the missed detection probability used in the protection level computation have been set as a function of the ICAO requirements reported in Table 2.
For APV phases of flight, the Integrity Risk must be divided into an horizontal and a vertical contribution. SBAS allocation has been used which assigns 98% for the vertical and 2% for the horizontal.

	APV Single constellation	APV Dual constellation
Missed detection probability	0.048	0.0226
False detection rate	1.6.10-5/test	1.6.10-5/test
Rare normal performance rate	<2x10-7/app	<2x10-7/app
Failed exclusion probability	0.048	0.0226
HAL	40 m	40 m
VAL	50 m (APV I) 20 m (APV II)	50 m (APV I) 20 m (APV II)

Table 2: Integrity monitoring parameter assumptions.

Detection/exclusion performance

To assess the detection/exclusion capability of the considered algorithms, a failure has been introduced on one of the GNSS measurements at time t_f=738s. The type and amplitude of the failure is determined by ICAO recommendations in appendix R to DO229. Each algorithm has been run N=20 times, each run corresponding to a different realization of the measurement noise so as to compute mean detection/exclusion performance indicators in the form of:

- the mean detection/exclusion delay,

$$\bar{\tau} = \frac{1}{N}\sum_{i=1}^{N}\left|t_{d/e}^{i} - t_f\right|,$$

where $t_{d/e}^{i}$ is either the detection or exclusion time for the i[th] run.

- the mean error size at detection/exclusion,

$$\delta\bar{x} = \sqrt{\frac{1}{N}\sum_{i=1}^{N}\left(x_{t_{d/e}^{i}} - \hat{x}_{t_{d/e}^{i}}\right)^{T}\left(x_{t_{d/e}^{i}} - \hat{x}_{t_{d/e}^{i}}\right)},$$

where x and $\hat{x}$ are vectors containing the actual and estimated position coordinates of the mobile, respectively. The obtained values are given in Table 4 at the end of the paper.

The GLR yields the smallest detection delays whatever the constellation and the type of error. As a result, the algorithm has the smallest error size at detection for the ramp error. As for the step error, the detection is instantaneous for the GLR and the RAIM but the latter achieves smaller error sizes at detection. This somewhat surprising result can be explained by the simulation setting. When using the RAIM, the position is computed by the hybridization filter after the FDE by using only the measurements monitored fault-free. It follows that when the failure is detected and excluded at once, it has no impact on the positioning error.
The comparison between the MSS and the RAIM should be discussed furthest. In the case of a small amplitude

error, the MSS outperforms the RAIM for GPS L1 constellation. On the contrary, when dual frequency measurements are considered, it takes on average longer for the MSS to detect the failure. Indeed, in this case, the measurement noise is small enough to make RAIM detection easy whereas the MSS is hindered by its implementation: its detection step is based on one measurement less than the RAIM. Besides, the correlated GNSS measurement error sources have been included in the state vector to preclude false detections. The price to pay for this increased robustness is that the estimation problem is more difficult to solve.

The same remarks hold for the exclusion performance whose results are presented on Table 5 at the end of the paper. It should be noted that for the proposed GLR algorithm the detection and exclusion are performed at the same time, hence the good exclusion performance of this approach.

Availability

The availability performance is analyzed by computing the protection levels of the Galileo-GPIRS GLR, the Galileo-GPIRS MSS and the GNSS RAIM all along the flight path and then comparing them to the alert limit specifications. The provided availability results should thus be understood as percentage of time of the whole flight duration when the HPL, respectively the VPL, compares favorably with the HAL, respectively the VAL provided in Table 2.

Fig 2 shows the values of the protection levels all along the flight trajectory for the GLR and the MSS algorithm. The RAIM HPL and VPL are not represented since they are on average greater than the MSS ones. Fig2 shows that the GLR significantly decreases the values of the protection levels, especially in the case of mono-frequency GPS. The corresponding availability results are reported in table 6 at the end of the paper.

It follows that the GLR exhibits the best results in terms of availability. Only in the case of standalone GPS L1 the algorithm performance is not compliant with civil aviation requirements. As for the MSS and the RAIM, the same explanations hold as for the detection/exclusion capability.

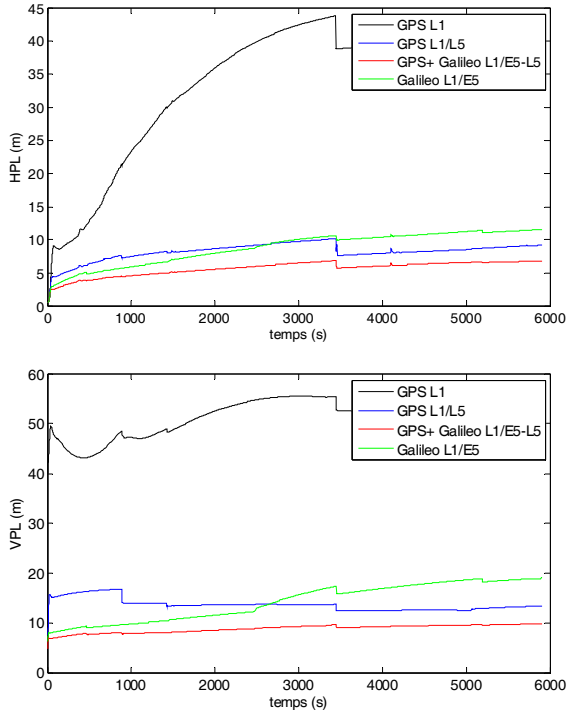

Fig 2. GLR Protection levels.

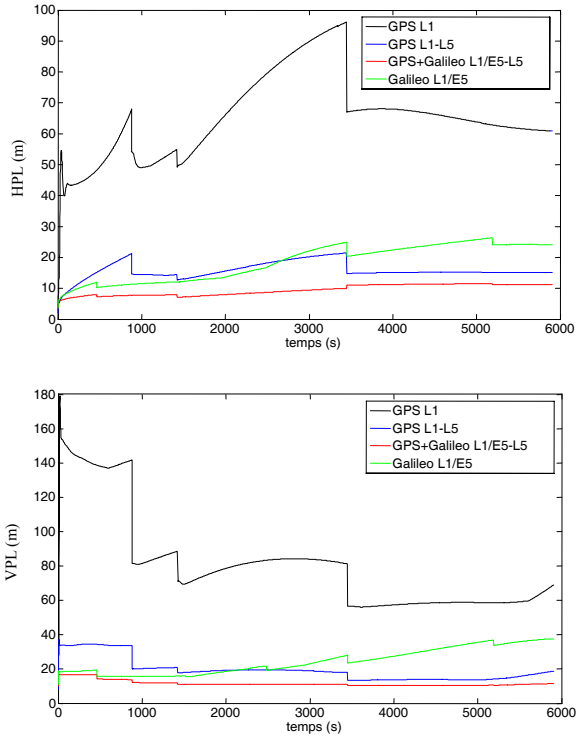

Fig 3. MSS Protection levels.

Two failures detection/exclusion

Finally, we have carried out additional simulations to emphasize the GLR ability to detect 2 simultaneous failures. For that purpose, 2 ramp failures of slope 2.5m/s have been introduced at time t=738s on 2 of the GPS pseudoranges so as to study the behavior of the algorithm. Here the one failure test and the two failures tests are run in parallel. The algorithm identifies the proper assumption and detects and excludes the failure source(s), as selecting the direction(s) of the largest test variable.
As for the single failures scenarios, the results obtained for 20 runs of the algorithm have been averaged to obtain the values reported in Table 5. It should be noticed that no misidentification (between the one failure and two failures assumptions) or missed detection has been observed all along the runs.

Constellation		Estimated failure amplitude	Mean detection delay	Mean error size at detection
GPS L1	SAT1	2.79 m/s	10.57s	3.62m
	SAT2	2.62 m/s		
GPS L1/L5	SAT1	2.72 m/s	5.17s	1.5m
	SAT2	2.55 m/s		

Table 3: GLR two failures detection.

CONCLUSION

This paper proposes to use the GLR algorithm to perform AAIM FDE. This approach has the advantage of being less computationally intensive than existing integrity monitoring schemes. Furthermore, the GLR can naturally cope with simultaneous multiple failures and is also well suited to detect small errors that would contaminate little by little the estimation filter outputs. However its application to civil aviation is not straightforward so that a few improvements are necessary. Therefore, we have extended the classical GLR formulation from step to ramp errors and we have also put forward a solution to identify and exclude the faulty measurements. Finally, a protection level formula has been developed that takes into account the error growth before detection.
The good performance of the proposed GLR AAIM algorithm based on GPS-Galileo/IRS tightly coupling has been emphasized through numerous simulation results. In particular, for the simulations run, the GLR is shown to improve FDE availability and to decrease on average the detection and exclusion delays in comparison to a Solution Separation AAIM and a weighted-LSR RAIM solutions that have been implemented:

- The GLR test affords better availability whatever the configuration of signals.
- It achieves on average smaller detection and exclusion delays than the GNSS RAIM and GNSS-IRS MSS.
- The GLR structured test allows for the detection and the exclusion of one as well as two simultaneous range failures without increasing the number of Kalman filters to run in parallel.

REFERENCES

[1] Integrated GPS/inertial detection availability- M. Brenner - Journal of The Institute of Navigation, Vol. 43, No. 2, Summer 1996.
[2] Navigation System With Solution Separation Apparatus For Detecting Accuracy Failures - M. Brenner - June 2, 1998,United States Patent #5,760,737.
[3] Minimum Operational Performance Standards for Global Positioning System / Wide Area Augmentation System Airborne Equipment
DO 229-D update FRAC - RTCA paper No 093-06/SC159-939, 2006
[4] FDE Using Multiple Integrated GPS/Inertial Kalman Filters in the Presence of Temporally and Spatially Correlated Ionospheric Errors – K.Vanderwerf – ION GPS 2001, Salt Lake City, UT.
[5] GPS/IRS AIME: certification for sole means and solution to RF interference Journal of The Institute of Navigation - J. Diesel, G. Dunn – Journal of The Institute of Navigation, Sept. 17-20 1996.
[6] A Generalized Likelihood Ratio approach to the detection of mean jumps in linear systems – A.S. Willsky - IEEE Transactions on Automatic Control, pp 108-112, 1976.
[7] Testing statistical hypothesis - E.L. Lehmann - Statistical/Probability series - Wadsworth & Brooks/Cole – 1991.
[8] On integrity monitoring of integrated navigation systems - J. Palmqvist - Thesis No. 600, Linköping Studies in Science and Technology, 1997
[9] The Global Positioning System and Inertial Navigation - J.A. Farrell, M. Barth - Mac Graw Hill, 1998.
[10] Investigation of Extending receiver Autonomous Integrity Monitoring (RAIM) to Combined Use of Galileo and Modernized GPS – Y.C. Lee – ION GNSS 2004, Long Beach, CA

Algorithm		MSS		GLR		RAIM	
Constellation		1	2	1	2	1	2
Ramp error 0.75m/s	Mean detection delay	91.48	43.17	23.7	20.27	97.42	29.95
	Horizontal error at detection	29.46	14.98	6.38	5.05	33.54	10.13
	Vertical error at detection	86.1	39.78	21.62	17.25	91.11	29.18
Step error 300 m	Mean detection delay	2.76	1	1	1	1	1
	Horizontal error at detection	27.58	21.03	2.75	1.2	2.23	1.18
	Vertical error at detection	42.73	31.20	11.51	5.71	5.51	4.39

Table 4 - Detection performance. Constellation 1: GPS L1, constellation 2: GPS L1/L5.

Algorithm		MSS		GLR		RAIM	
Constellation		1	2	1	2	1	83.55
Ramp error 0.75m/s	Mean detection delay	93.26	104.08	23.7	20.27	28.08	29.95
	Horizontal error at detection	30.29	34.34	6.38	5.05	77.20	10.13
	Vertical error at detection	87	93.30	21.62	17.25	1	29.18
Step error 300 m	Mean detection delay	2.81	2.06	1	1	1.18	1
	Horizontal error at detection	28.07	22.67	2.75	1.2	4.39	1.18
	Vertical error at detection	43.22	39.66	11.51	5.71	83.55	4.39

Table 5 - Exclusion performance. Constellation 1: GPS L1, constellation 2: GPS L1/L5.

Algorithm		GLR				MSS				RAIM			
Constellation		1	2	3	4	1	2	3	4	1	2	3	4
APV I	Horizontal	84.2%	100%	100%	100%	0%	100%	100%	100%	0%	100%	100%	100%
	Vertical	48%	100%	100%	100%	0%	100%	100%	100%	27%	99%	100%	100%
APV II	Horizontal	84.2%	100%	100%	100%	0%	100%	100%	100%	0%	100%	100%	100%
	Vertical	0%	100%	100%	100%	0%	76.2%	100%	38.7%	0%	74%	100%	100%

Table 6: Percentage of time for which the algorithms are compliant with APV requirements.Constellations : (1) GPS L1, (2)GPS L1-L5, (3) Galileo+GPS L1-E5/L5, (4) Galileo E5.